UCRL-JC-132560
PREPRINT

Multilayer Coatings of 10X Projection Optics for Extreme-Ultraviolet Lithography

C. Montcalm
E. Spiller
M. Wedowski
E. M. Gullikson
J. A. Folta

This paper was prepared for submittal to the
24th Annual International Symposium on Microlithography
Santa Clara, California
March 14-19, 1999

March 9, 1999

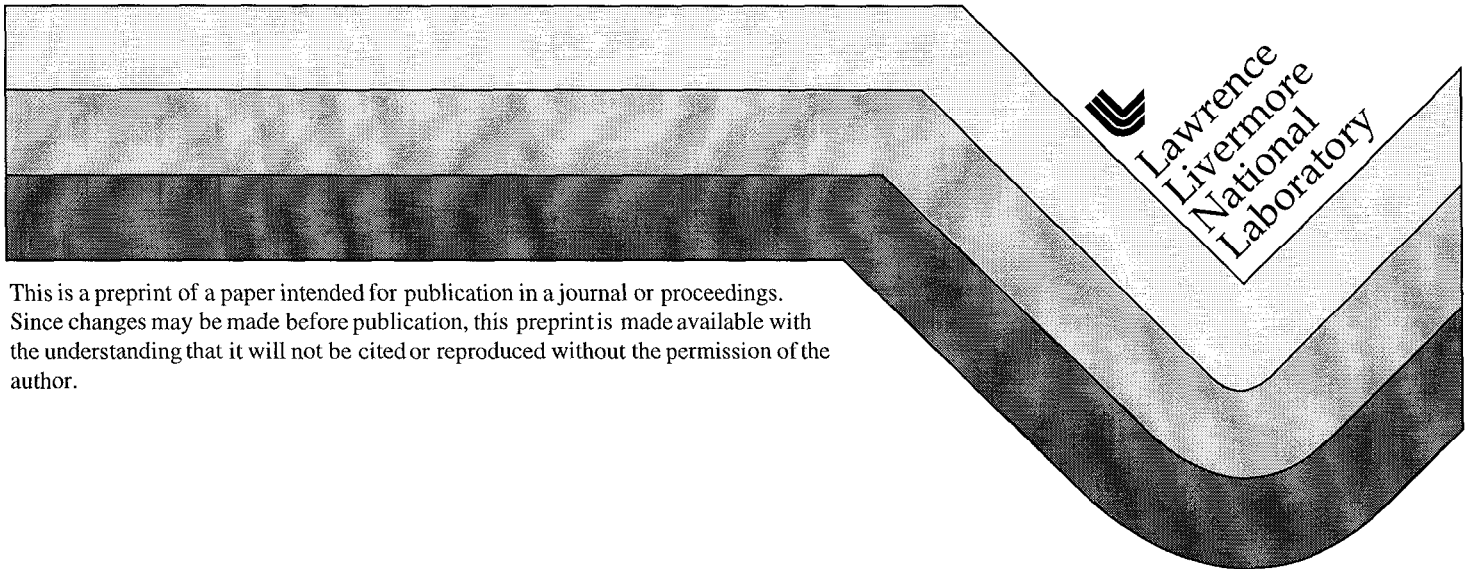

Multilayer coatings of 10X projection optics for extreme-ultraviolet lithography

Claude Montcalm,[†a] Eberhard Spiller,[a] Marco Wedowski,[a] Eric M. Gullikson,[b] and James A. Folta[a]

[a]Information Science and Technology
Lawrence Livermore National Laboratory
P.O. Box 808, L-395, Livermore, California 94551

[b]Center for X-Ray Optics
Lawrence Berkeley National Laboratory
1 Cyclotron Road, Berkeley, California 94720

ABSTRACT

Two new sets of projection optics for our prototype 10X reduction EUV lithography system were coated with Mo/Si multilayers. The coating thickness was graded across the optics by using shadow masks to ensure maximum throughput at all incidence angles in the camera. The overall deviation of the (normalized) wavelength response across the clear aperture of each mirror is below 0.01% RMS. However, the wavelength mismatch between two optics coated in different runs is up to 0.07 nm. Nevertheless, this is still within the allowed tolerances, and the predicted optical throughput loss in the camera due to such wavelength mismatch is about 4%. EUV reflectances of 63-65% were measured around 13.40 nm for the secondary optics, which is in good agreement with the expected reflectance based on the substrate finish as measured with AFM.

Keywords: Extreme ultraviolet (EUV) lithography, reflective coatings, multilayer deposition, graded coatings.

1. INTRODUCTION

The 10X Microstepper is currently the main laboratory tool to test exposure and processing steps for EUV lithography.[1] This EUV reduction camera evolved from a Schwarzschild optical system originally coated at (then) AT&T Bell Laboratories.[2] However, the figure errors of the original optics were too large to achieve diffraction-limited performance. Last year, two new sets of optics were fabricated and multilayer coated.[3] These optics benefited from recent advances in interferometry and aspheric polishing techniques[4] and mirrors with RMS figure errors as low as 0.6 nm were obtained. However, while the mirrors had excellent figure, they had considerable mid- and high-spatial frequency roughness.[5] The mid-spatial frequency roughness caused flare within the field of the camera, which significantly reduced the contrast, and the high-spatial frequency roughness caused scattering of the light outside the field of the camera, which reduced the optical throughput of the camera. It was therefore decided to fabricate two new sets of optics that would meet both the requirements of high quality figure and surface finish simultaneously. In this paper we describe the procedure used to coat the optics and to characterize their specular reflectance properties. Other papers in these proceedings describe in more detail the scattering and imaging properties of these mirrors.[1,6,7]

[†] C. Montcalm (correspondence): E-mail: montcalm@llnl.gov; Telephone: 925-424-2903; Fax: 925-422-8761

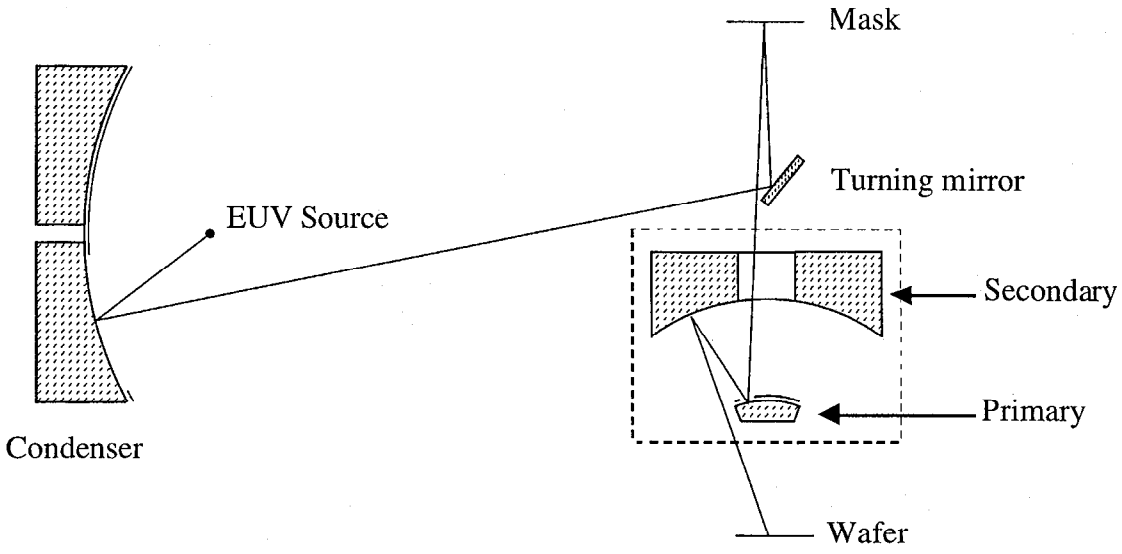

Figure 1. Layout of the optical system of the 10X Microstepper

2. MULTILAYER COATINGS SPECIFICATIONS

The layout of the optical system is given in Fig. 1. The major subsystems of this EUV camera were described in detail in a previous publication.[8] Each optic in this optical system is coated with a multilayer designed for maximum reflectance at near-normal incidence for a wavelength of 13.4 nm, except for the turning mirror that is designed for an incidence angle near 45°. Only the two spherical mirrors of the Schwarzschild objective that constitute the 10X-reduction projection system were upgraded. The primary (small) optic has a diameter of 16 mm and is convex with a 35-mm radius of curvature. The secondary (big) optic has a diameter of 90 mm and is concave with a 109-mm radius of curvature. Only an off-centered part of each optic is illuminated (clear aperture). The clear apertures consist of circular areas of 4.4 mm in diameter centered at 5.3 mm from the optical axis for the primary and 23.7 mm in diameter centered at 28.8 mm from the optical axis for the secondary. The clear apertures define a numerical aperture NA of 0.088.

The multilayer coatings specifications were described in detail elsewhere[2,3] and only a brief summary is given here. Geometrical ray tracing provides the range of incidence angles for different rays at each mirror, which are plotted versus radial distance from the optic axis at each mirror in Fig. 2(a). The following generalized Bragg law expresses the maximum peak reflectance condition,

$$\lambda = 2\Lambda \cos\alpha \sqrt{1 - \frac{2\bar{\delta}}{\cos^2\alpha}} \qquad (1)$$

which relates the incident angle α (from normal), the bilayer thickness Λ, and the wavelength λ of peak reflectance. Given the range of incidence angle and the operating wavelength of 13.4 nm, the bilayer thickness of the coating on each mirror must therefore be graded as shown in Fig. 2(b). The above equation accounts for refraction effects to the first order by incorporating the weighted average decrement of the refraction index $\bar{\delta}$ (i.e., $1-\bar{n}$), which was set to 0.0272 as an estimate for a Mo/Si multilayer mirror designed for 13.4 nm. Inaccuracies in this initial approximation are compensated for after the first set of surrogates are coated and their reflectance peak position is measured at-wavelength (Section 3.2).

The requirements on the control of the thickness distribution are driven by the need to both maximize optical throughput and minimize wavefront distortions. The scale for tolerable deviations of the deposited bilayer thickness from the ideal prescription given in Fig. 2(b) stems from the finite width of the reflectance peak (see Fig. 5 for an example of a typical reflectance curve). The multilayer coatings on each optic must be properly matched, so that the peak wavelength corresponding to successive reflections will coincide. Simulations show that a mismatch of ±0.05 nm in the reflectance peak position reduces the optical throughput by less than 2% and produces a phase error of only 1/20th of a wave, which is

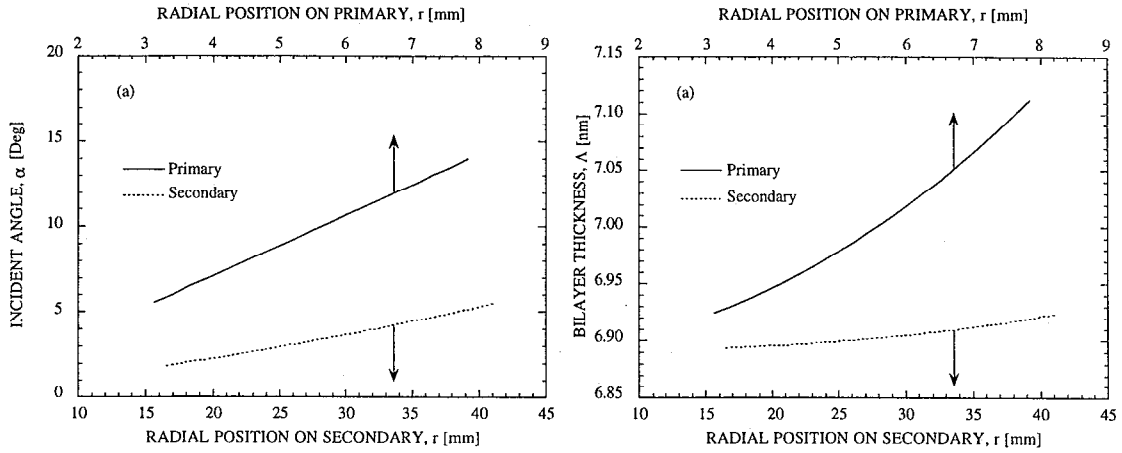

Figure 2. (a) Variation of the incident angle across the surface of each optic as a function of the distance from the optic axis at the mirror position. (b) Desired bilayer thickness Λ variation obtained from the generalized Bragg condition for $\lambda = 13.4$ nm.

significantly smaller than those produced by the figure errors of the actual optics. We therefore selected $\Delta\lambda = \pm 0.05$ nm or $\Delta\lambda/\lambda \cong \Delta\Lambda/\Lambda \cong \pm 0.4\%$ as the maximum tolerable deviations for the deposited bilayer thickness. As will be seen, the equivalence between the normalized reflectance peak wavelength $\Delta\lambda/\lambda$ and the normalized bilayer thickness $\Delta\Lambda/\Lambda$ is important because. Indeed, although it is the bilayer thickness that is specified by Eq. (1) and Fig. 2(b), it is the reflectance peak position that can be measured with the required precision and accuracy using synchrotron radiation.

3. EXPERIMENTAL PROCEDURES

The optics were coated with DC-magnetron sputtering using shaped masks to obtain the desired thickness profiles. The thickness distribution was measured using a synchrotron-based EUV reflectometer. The equipment and procedures used to perform the deposition and characterization are described here.

3.1 Multilayer deposition

The Mo/Si multilayers were deposited with a newly upgraded DC-magnetron sputtering system.[9] The system contains two 12.7 x 25.4 cm rectangular sputter sources placed 180° apart, i.e., at diametrically opposite sides of a circular chamber, with chimneys that limit the deposition region to the area directly above them. Two substrates located 90° apart are held face down on a rotating table (platter) at a distance of 6 cm above the sources in a "sputter-up" configuration. The sputter chamber is typically cryo-pumped until the pressure is in the low 10^{-7} Torr range. Ultrahigh purity Ar at pressure of 1.00 mTorr is used to sputter the Si and Mo targets at source powers of 360 and 170 W, respectively.

The multilayers are deposited by sweeping the substrates above the sources with a controlled rotation of the platter. A bilayer is deposited with each complete revolution of the platter. The layer thicknesses are determined by the time the substrate is exposed to the source which, in turn, depends on the substrate transit velocity. To achieve the desired thickness gradient, a precisely shaped shadow mask was carefully placed in front of the substrates spinning around their axis of symmetry. The arrangement of the substrates and the sputter sources is such that at any given time only one substrate is over a source and being coated. Therefore, both the primary and secondary could be coated in the same deposition run, which was helpful in obtaining a good wavelength matching between the optics.

The shadow masks were made of 0.5-mm thick aluminum metal sheet and cut with a computer numerical controlled (CNC) milling machine. The design process of the masks was similar to that described by Windt *et al.*[2] The proper shape of the mask is obtained through an iterative process: (1) a deposition is made with a shaped mask, (2) the thickness variation is measured along a radius, and (3) the thickness departure from ideal is used to calculate the new desired width of the mask at each radial point. With our deposition system, the coatings are generally too thin toward the outside edge of the optics when

no mask is used. Therefore, the final masks were such that a larger proportion of the inner part of the optics was shadowed. The masks were conformed by pressing them in a mandrel assembly with the same contour as the mirror to be coated. The masks were mounted to within 0.5 mm of the optic surface and extreme care was taken to ensure reproducibility of the positioning.

3.2 Multilayer reflectance and thickness distribution characterization

The mirrors were characterized by measuring their reflectance *versus* wavelength around 13.4 nm at different radii for a fixed angle of incidence. These measurements were performed using the Standard and Calibration Beamline of the Center for X-Ray Optics (beamline 6.3.2) at the Advanced Light Source (ALS).[10] This reflectometer uses a variable space grating monochromator that provides a spectral range extending from 1 nm to 25 nm (50 to 1300 eV) with a resolution ($\Delta\lambda/\lambda = \Delta E/E$) of up to 3000. A Si filter and an order sorter, consisting of a set of three grazing incidence mirrors, are used to further improve the spectral purity of the radiation. With this instrument, it is possible to measure the absolute reflectance and the centroid wavelength with a precision of ±0.2% (relative) and ±0.002 nm, respectively.

The reflectance measurements were performed at a fixed angle of incidence α_0 of 10° for the primary and 4° for the secondary. These angles simply correspond to the average angle of incidence each optic is illuminated in the optical system. The optics are illuminated at exactly these angles at radii r_0 of 5.38 mm and 32.27 mm of the actual primary and secondary optics, respectively. In the following section, the peak position *versus* radial position curves are normalized to the peak position value λ_0 measured at those r_0 radial positions. Therefore, the normalized curves go through 1.000 at $r_0 = 5.38$ mm and $r_0 = 32.27$ mm for the primary and the secondary, respectively.

The thickness profile of each coated optic was typically characterized along two perpendicular diameters (vertical and horizontal scans). In all cases, for a given diameter scan, the results from one side of the optic relative to the center (negative radii) were "folded" on top of the results from the other side (positive radii). This way, the radial symmetry of the coating could easily be checked.

4. RESULTS

We have coated the mirrors for two new sets of Schwarzschild projection optics for the 10X Microstepper system. We focused our effort in meeting the following two criteria: first, the coating thickness distribution, which we obtained with shadow masks, and second, the wavelength matching between the optics. The following sub-sections describe our achievements in these two respective areas. The reflectance properties of the mirrors are also briefly discussed.

4.1 Coating thickness distribution

Two sets of actual optics were coated after meeting the thickness distribution and reflectance peak position specifications on surrogates. Figures 3(a) and 3(b) show the resulting thickness profiles for the first set of projection optics for two different perpendicular diameters on the parts (vertical and horizontal diameters). The solid lines represent the targeted prescriptions; the data points are the measured values; and the dashed lines represent the boundaries of a ±0.4% tolerance zone. The overlap of the measured thickness profile on the desired profile is nearly perfect, especially for the primary. The overlap is exactly the same for both measured diameters confirming the radial symmetry of the coating thickness. The deviations from the desired profile accumulate to about 0.17% peak-to-valley (P-V) (0.06% RMS) and 0.71% P-V (0.16% RMS) for the primary and secondary, respectively. For the secondary, the deviations may appear large, but these occur mainly at the extremities of the clear aperture (near the center and the edge of the optic), where the illuminated area is only a small fraction of the total area. In fact, when these deviations are weighted by the length of the arc within the clear aperture for a given radial position, the calculations show that the average RMS deviation is only about 0.002%! This level of error in the coating thickness distribution is negligible and does not affect the imaging properties of the optical system.[1]

As shown in Figs. 4(a) and 4(b), the coatings made on the second set are nearly as high in quality as the first set (only one diameter was measured for this secondary). Once again, the radial symmetry of the coating thickness is confirmed by the overlap of the curves obtained from different diameters. The deviations from the desired profile accumulate to about 0.56% P-V (0.14% RMS) and 0.59% P-V (0.14% RMS) for the primary and secondary, respectively. The weighted average of the RMS deviations is only 0.003%.

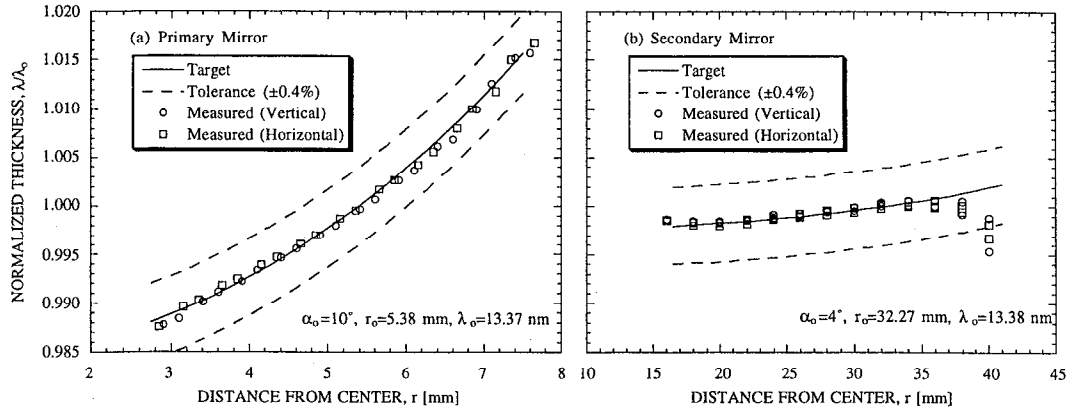

Figure 3. Thickness gradient of multilayers deposited on the first set of projection optics for the 10X Microstepper. Figures 3(a) and 3(b) represent the primary and secondary mirrors of the Schwarzschild system, respectively. The solid line is the target value, the dashed lines represent the boundaries of the allowed tolerances, and the symbols are the measured values for two perpendicular diameters.

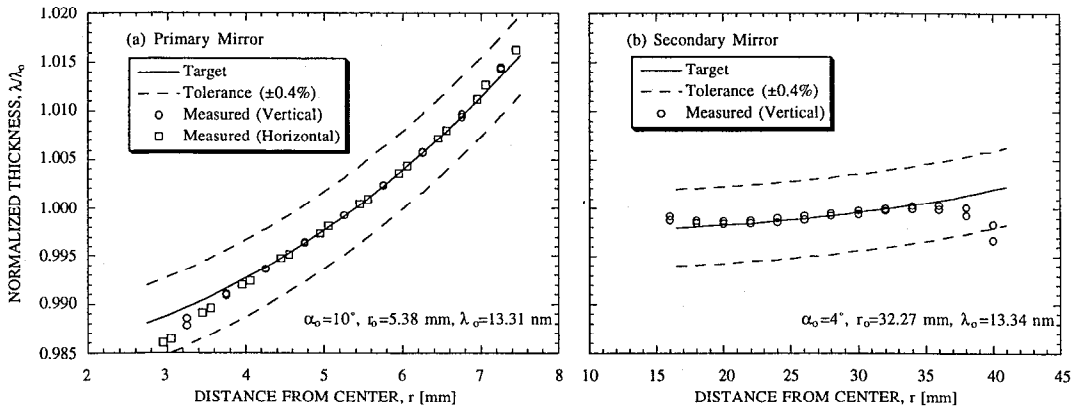

Figure 4. Thickness gradient of multilayers deposited on the second set of projection optics for the 10X Microstepper. Figures 4(a) and 4(b) represent the primary and secondary mirrors of the Schwarzschild system, respectively. The solid line is the target value, the dashed lines represent the boundaries of the allowed tolerances, and the symbols are the measured values for two perpendicular diameters.

The two sets of data for each type of optic (primary and secondary) show that we can reproduce the thickness profile from one deposition run to another within a 0.1% error when the same mask is used. This is about a factor of 8 better than the present specifications. The absolute value of the multilayer thickness, however, showed larger variations from run to run. Each curve in Figs. 3 and 4 were normalized by the centroid reflectance peak position λ_o of 13.37 nm and 13.38 nm, and 13.31 nm and 13.34 nm, for the primary and secondary of the first and second sets, respectively. This indicates that the reflectance peaks of two optics coated in the same deposition runs are offset by 0.03 nm, and can be offset by up to 0.07 nm when deposited in separate runs. The effect of this wavelength mismatch on the optical throughput is discussed in more detail in the following sub-section.

4.2 Reflectance and wavelength matching

Both the specular reflectance and diffuse scattering properties of the secondaries were measured. The diffuse scattering properties are described in detail by Gullikson *et al.*[6] and will not be discussed here. Also, the *absolute* reflectance of the two primaries was not measured because their highly convex shape diverges the reflected beam too much to be fully collected by the detector in our EUV reflectometer. A reflectance measurement on a primary optic can accurately show the peak position but not the absolute reflectance.

The specular reflectance curves of both secondaries are shown together in Fig. 5. Peak reflectances of 65.4% at 13.42 nm and 63.1% at 13.38 nm were measured for the mirrors of the first and second set, respectively. The reflectance of the secondary #2 is lower by 2.3% (absolute). Diffuse scattering measurements showed that this is consistent with a poorer surface finish quality in the high-spatial frequency range for this secondary #2.[6] The lost reflectance could be found in the off-specular scattering portion of the reflected beam. This higher level of surface roughness was later confirmed with atomic force microscopy (AFM) which showed a large number of 100-nm size particles over-coated by the multilayer. These particles are most likely residual polishing grit that was not removed completely by our optics cleaning procedure. We have since improved our optics cleaning procedure.

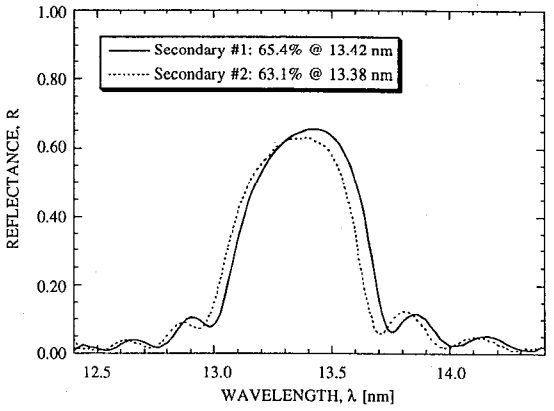

Figure 5. Specular reflectance curves for the secondary optics.

The two reflectance curves are shifted from each other by about 0.04 nm, due to an imperfect run-to-run repeatability. Wavelength-mismatched optics reduce the optical throughput of a system with multiple reflections. Figure 6 shows how the optical throughput of the 2-bounce 10X Microstepper projection optic assembly is reduced as the optic-to-optic mismatch increases. The optical throughput loss due to wavelength mismatch is less than 1% for a pair coated in the same deposition run ($\Delta\lambda \leq 0.03$ nm), but is about 4% for a pair coated in different deposition runs ($\Delta\lambda \leq 0.07$ nm). This slight mismatch is within the tolerance for the 10X Microstepper—it did not prevent Goldsmith *et al.*[1] from using the optics pair with the maximum wavelength mismatch to print high quality EUV lithography images. For the 10X Microstepper system, it was more important to maximize the image quality than to maximize the optical throughput.

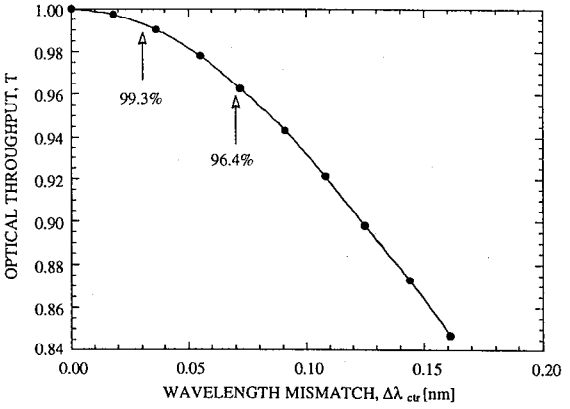

Figure 6. Predicted optical throughput of the 2-bounce 10X Microstepper projection optic assembly as a function of the optic-to-optic wavelength mismatch.

5. SUMMARY

Two new sets of projection optics for the 10X Microstepper were coated with Mo/Si multilayers. The coating thickness was graded across the optics such that all rays at the incidence angles in the camera reflect at the same wavelength to within ±0.4%. This tolerance assures that the coatings do not degrade the imaging performance of the camera. Precision shaped shadow masks in front of the spinning mirrors produced the required thickness gradient profile. The thickness profile of all mirrors matched the required profile well within the allowed ±0.4% specification. The root-mean-square (RMS) deviation of the measured profile from the target was below 0.15% for all four optics. A more accurate calculation made over the entire clear aperture showed the average RMS deviation is negligible, i.e., below 0.01% for all optics. The reflectance peak positions of the coated optics, which depend on the absolute value of the multilayer thickness, were spectrally matched to within 0.03 nm for the pairs coated in the same deposition run, and within 0.07 nm for all four optics. The predicted optical throughput loss in the camera due to a mismatch of 0.03 nm in the reflectance peak position is less than 1%, and is about 4% for a mismatch of 0.07 nm. This is within tolerance for the 10X Microstepper and will reduce the optical throughput by 4% at most. The average position of the reflectance peak maximum is located at a wavelength of 13.40 nm, exactly the targeted wavelength. EUV reflectances of 63–65% were measured for the secondary optics, which is in good agreement with the expected reflectance based on the substrate finish as measured with AFM.

6. ACKNOWLEDGMENTS

The authors would like to thank F. R. Grabner, M. A. Schmidt and G. B. Wells for their assistance in the maintenance and operation of the multilayer deposition systems. The authors also acknowledge the support of S. L. Baker in the AFM measurements and F. J. Weber for sharing his experience in the fabrication and use of shadow masks for this kind of multilayer coatings. This work was performed under the auspices of the U. S. Department of Energy by the Lawrence Livermore National Laboratory under Contract No. W-7405-ENG-48. Funding was provided by the Extreme Ultraviolet Limited Liability Company (EUV LLC) under a Cooperative Research and Development Agreement.

7. REFERENCES

1. J.E.M. Goldsmith, K.W. Berger, D.R. Bozman, G.F. Cardinale, D.R. Folk, C.C. Henderson, D.J. O'Connell, A.K. Ray-Chaudhuri, K.D. Stewart, D.A. Tichenor, H.N. Chapman, R.J. Gaughan, R.M. Hudyma, C. Montcalm, E.A. Spiller, J.S. Taylor, J.D. Williams, K.A. Goldberg, E.M. Gullikson, P. Naulleau, and J.L. Cobb, "Sub-100-nm imaging with the EUV 10x Microstepper," in these proceedings.
2. D.L. Windt and W.K. Waskiewicz, "Multilayer facilities required for extreme-ultraviolet lithography," J. Vac. Sci. Technol. B **12**, 3826-3832 (1994).
3. E. Spiller, F.J. Weber, C. Montcalm, S.L. Baker, and E.M. Gullikson, "Multilayer coating and tests of a 10X extreme ultraviolet lithography camera," in *Emerging Lithographic Technologies II*, Y. Vladimirsky, Ed., Proceedings of SPIE Vol. **3331**, 62-71 (1998).
4. J.S. Taylor, G.E. Sommargren, D.W. Sweeney, and R.M. Hudyma, "Fabrication and testing of optics for EUV projection lithography," in *Emerging Lithographic Technologies II*, Y. Vladimirsky, Ed., Proceedings of SPIE Vol. **3331**, 580-590 (1998).
5. E.M. Gullikson, "Scattering from normal incidence EUV optics," in *Emerging Lithographic Technologies II*, Y. Vladimirsky, Ed., Proceedings of SPIE Vol. **3331**, 72-80 (1998).
6. E.M. Gullikson, S.L. Baker, J.E. Bjorkholm, J. Bokor, K.A. Goldberg, J.E.M. Goldsmith, C. Montcalm, P. Naulleau, E.A. Spiller, D.G. Stearns, J.S. Taylor, and J.H. Underwood, "EUV scattering and flare of 10X projection cameras," in these proceedings.
7. K.A. Goldberg, P. Naulleau, H.N. Chapman, R.J. Gaughan, and J. Bokor, "Direct comparison of EUV and visible light interferometries," in these proceedings.
8. D.A. Tichenor, G.D. Kubiak, S.J. Haney, R.P. Nissen, K. W. Berger, R.W. Arling, A.K. Ray-Chaudhuri, K.B. Nguyen, R.H. Stulen, J.B. Wronosky, J.D. Jordan, T. G. Smith, J.R. Darnold, P. M. Kahle, A.A. Jojola, S. M. Kohler, R.S. Urenda, D.R. Wheeler, J.E. Bjorkholm, O.R. Wood, II, G.N. Taylor, and R.S. Hutton, "Recent results in the development of an integrated EUVL laboratory tool," in *Electron-beam, X-Ray, EUV, and Ion-Beam Submicrometer Lithographies for Manufacturing V*, J.M. Warlaumont, Ed., Proceedings of SPIE Vol. **2437**, 292-307 (1995).
9. J.A. Folta, S. Bajt, T.W. Barbee, Jr., F.R. Grabner, P.B. Mirkarimi, C. Montcalm, T. Nguyen, M.A. Schmidt, E. Spiller, C.C. Walton, and M. Wedowski, "Advances in multilayer reflective coatings for extreme ultraviolet lithography," in these proceedings.
10. J.H. Underwood and E.M. Gullikson, "Beamline for measurement and characterization of multilayer optics for EUV lithography," in *Emerging Lithographic Technologies II*, Y. Vladimirski, Ed., Proceedings of SPIE Vol. **3331**, 52-61 (1998).